



SPE 59300

## Control of Water Injection into a Layered Formation

Dmitriy B. Silin<sup>1</sup>, and Tad W. Patzek<sup>1,2,3</sup>

<sup>1</sup>Lawrence Berkeley National Laboratory; <sup>2</sup>University of California at Berkeley; <sup>3</sup>SPE Member, [patzek@patzek.berkeley.edu](mailto:patzek@patzek.berkeley.edu)

Copyright 2000, Society of Petroleum Engineers Inc.

This paper was prepared for presentation at the 2000 SPE/DOE Improved Oil Recovery Symposium held in Tulsa, Oklahoma, 3–5 April 2000.

This paper was selected for presentation by an SPE Program Committee following review of information contained in an abstract submitted by the author(s). Contents of the paper, as presented, have not been reviewed by the Society of Petroleum Engineers and are subject to correction by the author(s). The material, as presented, does not necessarily reflect any position of the Society of Petroleum Engineers, its officers, or members. Papers presented at SPE meetings are subject to publication review by Editorial Committees of the Society of Petroleum Engineers. Electronic reproduction, distribution, or storage of any part of this paper for commercial purposes without the written consent of the Society of Petroleum Engineers is prohibited. Permission to reproduce in print is restricted to an abstract of not more than 300 words; illustrations may not be copied. The abstract must contain conspicuous acknowledgment of where and by whom the paper was presented. Write Librarian, SPE, P.O. Box 833836, Richardson, TX 75083-3836, U.S.A., fax 01-972-952-9435.

### Abstract

In previously published work, we have analyzed transient injection of water from a growing vertical hydrofracture into a low-permeability compressible rock of uniform properties, filled with a fluid of identical mobility. Here we extend the prior analysis<sup>1</sup> to water injection into a layered rock initially filled with a fluid of different mobility. We then develop a new control model of water injection from a growing hydrofracture into a layered formation. Based on the new model, we design an optimal injection controller that manages the rate of water injection in accordance with the hydrofracture growth and the formation properties. As we have already demonstrated, maintaining the rate of water injection into low-permeability rock above a reasonable minimum inevitably leads to hydrofracture growth if flow in a uniform formation is transient. The same conclusion holds true for transient flow in layered formation. Analysis of field water injection rates and wellhead injection pressures leads us to conclude that direct links between injectors and producers can be established at early stages of waterflood, especially if injection policy is aggressive. On one hand, injection into a low-permeability rock is slow and there is a temptation to increase injection pressure. On the other hand, such an increase may lead to irrecoverable reservoir damage: fracturing of the formation and water channeling from the injectors to the producers. Such channeling may be caused by thin highly permeable reservoir layers, which may conduct a substantial part of injected water. Considering these field observations, we expand our earlier model. Specifically, we consider a vertical hydrofracture in contact with a multi-

layered reservoir where some layers have high permeability and they, therefore, quickly establish steady state flow from an injector to a neighboring producer.

The main part of this paper is devoted to the development of an optimal injection controller for purely transient flow and for mixed transient/steady-state flow into a layered formation. The objective of the controller is to maintain the prescribed injection rate in the presence of hydrofracture growth. Such a controller will be essential in our proposed automated system of field-wide waterflood surveillance and control. We design optimal injection controllers using methods of optimal control theory. The history of injection pressure and cumulative injection, along with estimates of the hydrofracture size are the controller input data. By analyzing these inputs, the controller outputs an optimal injection pressure for each injector. When designing the controller, we keep in mind that it can be used either off-line as a smart advisor, or on-line in a fully automated regime.

We demonstrate that the optimal injection pressure depends not only on the instantaneous measurements, but it is determined by the whole history of injection and growth of the hydrofracture. Because our controller is process-based, the dynamics of the actual injection rate and the pressure can be used to estimate an effective area of the hydrofracture. The latter can be passed to the controller as one of the input parameters. Finally, a comparison of the estimated fracture area with independent measurements leads to an estimate of the fraction of injected water that flows directly to the neighboring producers due to channeling or thief-layers.

### Introduction

Our ultimate goal is to design an integrated system of field-wide waterflood surveillance and supervisory control. As of now, this system consists of the Waterflood Analyzer<sup>2</sup> and a network of individual injector controllers, all implemented in modular software. In the future, our system will incorporate a new generation of microtiltmeters based on the micro-electronic-mechanical system (MEMS) sensors and other revolutionary technologies.

In this paper, we design an optimal controller of water injection into a low permeability rock from a growing vertical

hydrofracture. The objective of control is water injection at a prescribed rate, which itself may be a function of time. The control parameter is injection pressure. The controller is based on the optimization of a quadratic performance criterion subject to the constraints imposed by interactions among the injector, the hydrofracture and the formation. The inputs are the histories of wellhead injection pressure, cumulative volume of injected fluid, and area of the hydrofracture, see **Fig. 1**. The output, optimal injection pressure is determined not only by the instantaneous measurements, but also by the history of observations. With time, the system “forgets” distant past.

The wellhead injection pressures and rates are readily available if the injection water pipelines are equipped with pressure gauges and flow meters, and if the respective measurements are appropriately collected and stored as time series. It is now a common field practice to collect and maintain such data. The measurements of hydrofracture area are not as easily available. There are several techniques described in the literature. For example, references<sup>3,4</sup> and<sup>5</sup> develop a *hydraulic impedance* method of characterizing injection hydrofractures. This method is based on the generation of low frequency pressure pulses at the wellhead or beneath the injection packer, and on the subsequent analysis of the reflected acoustic waves. An extensive overview of hydrofracture diagnostics methods has been presented in Ref.<sup>6</sup>.

The direct measurements of hydrofracture area can be expensive. Moreover, for waterflood analysis it is important to know the area of contact between the injected water in the hydrofracture and the formation. It follows from the analysis of mechanical rock stresses<sup>7</sup> that the fracture is not filled with water up to its tips. This fact is readily confirmed by experiment<sup>8-10</sup>. Therefore, we define an effective fracture area as the area of injected water-formation contact in the hydrofractured zone. Clearly, a geometric estimate of the fracture size is insufficient to estimate this effective area.

In the present paper, we propose a model-based method of identification of the effective fracture area utilizing the system response to the controller action. In order to implement this method, one needs to maintain a database of injection pressures and cumulative injection. As noted earlier, such databases are now readily available and the proposed method does not impose extra measurement costs.

Earlier we proposed a model of linear transient incompressible fluid flow from a growing hydrofracture into low-permeability, compressible rock. A similar analysis can be performed for heterogeneous layered-rock. Our analysis of field injection rates and injection pressures leads to the conclusion that the injectors and producers may link very early in a waterflood. Consequently, we expand our water injection model to a multi-layered hydrofracture where in some layers steady-state flow develops between injector and

neighboring producer. As in Ref.<sup>1</sup>, we consider slow growth of the hydrofracture during water injection.

The control procedure is designed in the following way. First, we determine what cumulative injection (or, equivalently, injection rate) is the desirable goal. This decision can be made through an analysis of waterflood<sup>2</sup>, a reservoir simulation and from economical considerations. Second, by analyzing the deviation of actual cumulative injection from the target cumulative injection, and using the estimated fracture area, the controller determines injection pressure, which minimizes this deviation. Control is applied by adjusting a flow valve at the wellhead and it is iterated in time.

The convolution nature of our model prevents obtaining the optimal solution as a genuine feedback control and designing the controller as a standard closed-loop system. At each time, we have to account for the previous history of injection. However, the feedback mode may be imitated by designing the control on a relatively short interval that slides with time. When an unexpected event happens, e.g., a sudden fracture extension occurs, a new sliding interval is generated and the controller is refreshed promptly.

A distinctive feature of the controller proposed here is that it is model-based. Although we cannot predict *yet* when and how the fracture extensions happen, the controller automatically takes into account the effective fracture area changes and the decline of the pressure gradient caused by gradual saturation of the surrounding formation with injected water. The concept of effective fracture area implicitly accounts for the decrease of permeability caused by formation plugging.

The material in this paper is organized as follows. First, we review a modified Carter's model of transient water injection from a growing hydrofracture. We extend this model to incorporate the case of layered formation with possible channels or thief-layers. Second, we obtain a system of equations characterizing optimal injection pressure. Third, we elaborate on how this system of equations can be solved for different models of hydrofracture growth. Fourth, we obtain and compare three modes of optimal control: exact optimal control, optimal control produced by the system of equations, and piecewise-constant optimal control. Finally, we extend our analysis of the control model to the case of layered reservoir with steady-state flow in one or several layers.

### Modified Carter's Model

We assume the transient linear flow from a vertical hydrofracture through which an incompressible fluid (water) is injected into the surrounding uniform rock of low permeability. The flow is orthogonal to the fracture faces. The fluid is injected under a uniform pressure, which depends on time. Under these assumptions, the cumulative injection can be calculated from the following equation<sup>1</sup>:

$$Q(t) = wA(t) + 2 \frac{kk_r}{\mu\sqrt{\pi\alpha}} \int_0^t \frac{(p_{inj}(\tau) - p_i)A(\tau)}{\sqrt{t - \tau}} d\tau \dots\dots\dots(1)$$

Here  $k$  and  $k_r$  are, respectively, the absolute rock permeability and the relative water permeability in the formation outside the fracture, and  $m$  is the water viscosity. Parameters  $a$  and  $p_i$  denote the hydraulic diffusivity and the initial pressure in the formation. The effective fracture area at time  $t$  is measured as  $A(t)$  and its constant width is denoted by  $w$ . Thus, the first term on the right-hand side of Eq. (1) represents the volume of injected fluid necessary to fill up the fracture. This volume is small in comparison with the second term in Eq. (1). We assume that the permeability inside the hydrofracture is much higher than outside it, so at any time the drop of injection pressure along the fracture is negligibly small. We introduce  $A(t)$  as an effective area because the actual permeability may change in time due to formation plugging<sup>11</sup> and increase of water saturation. In addition, the injected water may not fill up entire fracture volume. Therefore,  $A(t)$  is not, in general, equal to the geometric area of the hydrofracture.

From Eq. (1) it follows that the initial value of the cumulative injection is equal to  $wA(0)$ . The control objective is to keep the injection rate  $q(t)$  as close as possible to a prescribed target injection rate  $q_*(t)$ . Since Eq. (1) is formulated in terms of cumulative injection, it is more convenient to formulate the optimal control problem in terms of target cumulative injection:

$$Q_*(t) = Q_*(0) + \int_0^t q_*(\tau) d\tau \dots\dots\dots(2)$$

If control maintains the actual cumulative injection close to  $Q_*(t)$ , then the actual injection rate is close to  $q_*(t)$  on average.

An implicit assumption in Eq. (1) is that both the injected water and the original formation fluid have similar properties. In the following section, we relax this hypothesis.

**Two different fluids**

In this section, we estimate the water-flooded reservoir volume when the original reservoir fluid has different properties than the injected water. Denote by  $k_w$ ,  $a_w$  and  $m_w$ , respectively, the relative permeability, hydraulic diffusivity, and viscosity of injected water; and by  $k_o$ ,  $a_o$  and  $m_o$ , the analogous properties of the reservoir fluid. As in<sup>1</sup>, we assume that the injection pressure changes according to

$$\begin{aligned} \frac{\partial p_\tau}{\partial t} &= \alpha \frac{\partial^2 p_\tau}{\partial x^2}, \quad t \geq \tau, \quad x \geq 0, \\ p_\tau(x, \tau) &= \begin{cases} p_{inj}(\tau), & x = 0, \\ p_i, & x > 0, \end{cases} \dots\dots\dots(3) \\ p_\tau(0, t) &= p_{inj}(t), \end{aligned}$$

where  $p_i(x, t)$  is the pressure in the formation in front of the part of the fracture opened at time  $t$ . In Ref.<sup>12</sup>, we elaborate on why Eq. (3) characterizes flow from a growing hydrofracture into a low-permeability formation. Our analysis is based on the Gordeyev and Entov self-similar solution of 2D transient flow<sup>13</sup>. The applicability of Eq. (3) is also confirmed in Ref.<sup>14</sup>. During the displacement of the reservoir fluid by injected water, the coefficient  $a$  in (3) is piecewise constant: it takes on the value  $a_w$  if  $0 \leq x \leq X(t, t)$ , and it is equal to  $a_o$  for  $x > X(t, t)$ . Here  $X(t, t)$  is the distance between the fracture and the surface of contact between the two fluids in formation in front of the part of the fracture opened at time  $t$ . Using approach similar to that in<sup>13</sup>, we obtain that if the injection pressure is constant,  $p_{inj}(t) \equiv p_{inj}$ , then the solution to Eq. (3) is provided by

$$p(t; t, x) = p_i + F(t; t, x)(p_{inj} - p_i) \dots\dots\dots(4)$$

where

$$F(t; t, x) = \begin{cases} \operatorname{erfc}\left(\frac{x}{2\sqrt{a_w(t-t)}}\right), & 0 \leq x \leq X(t, t) \\ \operatorname{erfc}\left(\frac{x}{2\sqrt{a_o(t-t)}}\right), & x > X(t, t) \end{cases} \dots\dots\dots(5)$$

For time-dependent injection pressure, Duhamel's theorem<sup>15,16</sup> yields

$$p(t; t, x) = p_i + \int_t^t \frac{\partial F(t; t-x, x)}{\partial t} (p_{inj}(x) - p_i) dx \dots\dots\dots(6)$$

Hence, we will have the solution as we find the function  $X(t, t)$ , or the distance of water penetration.

In order to find  $X(t, t)$  we need the mass balance of the fluids. The specific leak-off flow rate through the fracture surface is equal to

$$dq_t(t) = - \frac{kk_w}{m_w} \int_x p_t(0, t) dA(t) \dots\dots\dots(7)$$

where  $dA(t)$  is the increment of the fracture area at time  $t$  and  $k_w$  is the relative permeability of water. In order to

calculate the cumulative injection through the area  $dA(t)$  we integrate (7) from  $t$  to  $t$ . Then

$$X(\tau, t) = -\frac{kk_w}{\mu_w \phi} \int_{\tau}^t \frac{\partial p_i(0, \xi)}{\partial x} d\xi \dots\dots\dots(8)$$

where  $j$  is the porosity of the formation.

Now it remains to calculate the pressure gradient at the fracture surface. Since the open parts of fracture are surrounded by water, the gradient in Eq. (7) is determined by the hydraulic diffusivity of water, not of the reservoir fluid. Hence, the argument similar to<sup>1</sup> can be applied and

$$X(\tau, t) = \frac{kk_w}{\mu_w \phi \sqrt{\pi \alpha_w}} \int_{\tau}^t \left( \frac{p_{inj}(\tau) - p_i}{\sqrt{\eta - \tau}} + \int_{\tau}^{\eta} \frac{dp_{inj}(\xi) / d\xi}{\sqrt{\eta - \xi}} d\xi \right) d\eta \dots\dots(9)$$

Using Eq. (B.1) from<sup>1</sup> we eventually obtain

$$X(\tau, t) = \frac{kk_w}{\mu_w \phi \sqrt{\pi \alpha_w}} \int_{\tau}^t \frac{p_{inj}(\eta) - p_i}{\sqrt{\eta - \tau}} d\eta \dots\dots\dots(10)$$

In particular, if the injection pressure is constant,  $p_{inj}(t) \equiv p_{inj}$ , Eq. (10) reduces to

$$X(t, t) = \frac{kk_w (p_{inj} - p_i)}{2m_j \sqrt{\pi a_w}} \sqrt{t - t} \dots\dots\dots(11)$$

Another special case occurs if we assume that the fracture is symmetric, has rectangular shape with constant height and its half length grows as the square root of time:  $l(\tau) = l_0 + R\sqrt{\tau}$ , where  $l_0$  is the initial half length of the fracture and  $R$  is the fracture growth rate. Expressing  $\tau$  through  $l(\tau)$  and substituting into Eq. (13) yields

$$\frac{X(\tau, t)^2}{K^2} + \frac{l(\tau) - l_0^2}{R^2} = t \dots\dots\dots(12)$$

where

$$K = \frac{2kk_w}{\mu_w \phi \sqrt{\pi \alpha_w}} p_{inj} - p_i \dots\dots\dots(13)$$

**Carter's model for layered reservoir**

We assume transient linear flow from a vertical hydrofracture injecting an incompressible fluid into the surrounding formation. The flow is perpendicular to the fracture faces. The reservoir is layered and there is no cross-flow between the layers. Denote by  $N$  the number of layers and let  $h_i, i=1,2,\dots,N$ , be the thickness of each layer. Suppose that the hydrofracture intersects all the layers in proportion to their thickness, so that the area of the fracture in layer  $i$  is equal to

$$A_i(t) = \frac{h_i}{\sum_{j=1}^N h_j} A(t) \dots\dots\dots(14)$$

The injected fluid pressure  $p_{inj}(t)$  depends on time  $t$ . If the permeability and the hydraulic diffusivity of layer  $i$  are equal, respectively, to  $k_i$  and  $\alpha_i$ , then cumulative injection into layer  $i$  is given by the following equation<sup>1</sup>:

$$Q_i(t) = wA_i(t) + 2 \frac{k_i k_r}{\mu \sqrt{\pi \alpha_i}} \int_0^t \frac{p_{inj}(\tau) - p_{init}}{\sqrt{t - \tau}} A_i(\tau) d\tau \dots\dots(15)$$

Eq. (15) is valid only in layers with transient flow. The layers where steady-state flow has been established must be treated differently. The relative permeabilities  $k_r$  in the different layers may be different. Summing up for all  $i$ , and taking into account Eq. (14), Eq. (15) implies:

$$Q(t) = wA(t) + 2 \frac{K}{\mu \sqrt{\pi}} \int_0^t \frac{(p_{inj}(\tau) - p_{init}) A(\tau)}{\sqrt{t - \tau}} d\tau \dots\dots\dots(16)$$

where

$$K = \sum_{i=1}^N \frac{h_i}{\sum_{j=1}^N h_j} \frac{k_i k_r}{\sqrt{\alpha_i}} = \frac{1}{H} \sum_{i=1}^N h_i \frac{k_i k_r}{\sqrt{\alpha_i}} \dots\dots\dots(17)$$

is the thickness and hydraulic conductivity-averaged reservoir permeability. Here  $H$  is the injection interval thickness. Of course, the hydrostatic injection and reservoir pressures can be readily implemented in Eq. (16).

From Eq. (16) it follows that

$$\int_0^t \frac{p_{inj}(\tau) - p_{init}}{\sqrt{t - \tau}} A(\tau) d\tau = \frac{\mu \sqrt{\pi}}{2K} (Q(t) - wA(t)) \dots\dots\dots(18)$$

Therefore, the portion of injection entering  $i$ -th layer is

$$Q_i(t) = \frac{wh_i}{H} A(t) + \frac{k_i k_r h_i}{\sqrt{\alpha_i} HK} Q(t) \dots\dots\dots(19)$$

Now assume that all  $N$  layers fall into two categories: the layers with indices  $i \in I = i_1, i_2, \dots, i_r$  are in transient flow, whereas the layers with indices  $j \in J = j_1, j_2, \dots, j_s$  are in steady-state flow, i.e., a connection between the injector and producers has been established. By definition, the sets of indices  $I$  and  $J$  are disjoint and together yield all the layer indices  $\{1, 2, \dots, N\}$ . Since linkage is first established in the layer with highest permeability, one has

$$\min_{j \in J} kk_r_j > \max_{i \in I} kk_r_i \dots\dots\dots(20)$$

The flow rate in each layer from set  $J$  is given by

$$q_j(t) = \frac{k_j k_{r_j} A_j(t)}{\mu} \frac{p_{inj}(t) - p_{pump}(t)}{L} \dots\dots\dots(21)$$

Here  $L$  is the distance between the injector and a neighboring producer and  $p_{pump}(t)$  is the pressure at the producer. Here, for simplicity, we assume that all the flow paths connect the injector under consideration to the same producer. Such an assumption is natural as long as each layer is homogeneous. The total flow rate into the steady-state layers is

$$q_J(t) = \frac{p_{inj}(t) - p_{pump}(t)}{L} A(t) \sum_{j \in J} \frac{k_j k_{r_j} h_j}{\mu H} \dots\dots\dots(22)$$

Since circulating water from an injector to a producer is not desirable, we come to the following requirement:  $q_j(t)$  should not exceed an upper bound  $q_{adm}$ :  $q_j(t) \leq q_{adm}$ . Invoking Eq. (22), one infers that the following constraint is imposed on the injection pressure:

$$p_{inj}(t) \leq p_{adm}(t) \dots\dots\dots(23)$$

where the admissible pressure  $p_{adm}(t)$  is given by

$$p_{adm}(t) = p_{pump}(t) + \frac{q_{adm} L}{A(t) \sum_{j \in J} \frac{k_j k_{r_j} h_j}{\mu H}} \dots\dots\dots(24)$$

Eq. (24) leads to a very important conclusion. Earlier we have demonstrated that injection into a transient-flow layer is determined by a convolution integral of the product of the hydrofracture area and the difference between the injection pressure and initial formation pressure. In transient flow, the larger the hydrofracture area, the more fluid we can inject into the formation. In contrast, from Eqs. (22) and (24) it follows that as soon as channeling between injector and producer occurs, a larger fracture area increases the volume of water circulated from the injector to the producer. At the initial transient stage of waterflood, a hydrofracture plays a positive role, it helps to maintain higher injection rate and push more oil towards the producing wells. With channeling, the role of the hydrofracture is reversed. The larger the hydrofracture area, the more water is circulated between injector and producer. As our analysis of actual field data shows, channeling is almost inevitable, sometimes at remarkably early stages of waterflood. Therefore, it does matter how the initial hydrofrac job is done and how the waterflood is initiated. An injection policy that is too aggressive will result in a "fast start" of injection, but may cause severe problems later on, sometimes very soon.

**Control model**

In order to formulate the optimal control problem, we must pick up a performance criterion for the process described by (1). Suppose that we are planning to apply control on a time interval  $[\vartheta, T]$ ,  $T > \vartheta \geq 0$ . In particular, we assume that the cumulative water injection and the injection pressure are known on interval  $[0, \vartheta]$ , along with the effective fracture area  $A(t)$ . On interval  $[\vartheta, T]$ , we want to apply such an injection pressure that the resulting cumulative injection will be as close as possible to that given by Eq. (2). This requirement may be formulated in the following way:

*Minimize*

$$J[p_{inj}] = \frac{1}{2} \int_{\vartheta}^T w_q(t) Q(t) - Q_s(t) \text{ }^2 dt + \frac{1}{2} \int_{\vartheta}^T w_p(t) p_{inj}(t) - p_*(t) \text{ }^2 dt \dots\dots\dots(25)$$

*subject to constraint (1).*

The weight-functions  $w_p$  and  $w_q$  are positive-defined. They reflect the trade-off between the closeness of actual cumulative injection  $Q(t)$  to the target  $Q_s(t)$ , and the well-posedness of the optimization problem. For small values of  $w_p$ , minimization of functional (25) forces  $Q(t)$  to follow the target injection strategy,  $Q_s(t)$ . However, if the value of  $w_p$  is too small, then the problem of minimization of functional (25) becomes ill-posed<sup>17,18</sup>. Moreover, in the optimal control criterion derived below, the function  $w_p$  is in the denominator; therefore, computational stability of this criterion deteriorates as  $w_p$  approaches zero. At the same time, if we consider a specific mode of control, e.g., piecewise constant control, then the well-posedness of the minimization problem is not affected by  $w_p \equiv 0$ . Function  $p_*(t)$  defines a reference value of the injection pressure. Theoretically, this function can be selected arbitrarily; however, practically it should be a rough estimate of the optimal injection pressure. Below, we discuss the ways in which  $p_*(t)$  can be reasonably specified.

The optimization problem we have just formulated is a linear-quadratic optimal control problem. In the next section, we derive the necessary and sufficient conditions of optimality in the form of a system of integral equations.

**Optimal injection pressure**

Here we obtain the necessary and sufficient optimality conditions for problem (1)–(25). We analyze the obtained equations in order to characterize optimal control in two different modes: the continuous mode and the piecewise-constant mode. In addition, we characterize the injection pressure function, which provides exact identity  $Q(t) \equiv Q_*(t)$ ,  $\vartheta \leq t \leq T$ .

Put  $U(t) = p_{inj}(t) - p_*(t)$  and  $V(t) = Q(t) - Q_*(t)$ . Then the optimal control problem transforms into

Minimize

$$J = \frac{1}{2} \int_{\vartheta}^T w_q(t)V(t)^2 dt + \frac{1}{2} \int_{\vartheta}^T w_p(t)U(t)^2 dt \dots\dots\dots(26)$$

subject to

$$V(t) = -Q_*(t) + wA(t) + 2 \frac{kk_w}{\mu\sqrt{\pi\alpha}} \int_{\vartheta}^t \frac{p_{inj}(\tau) - p_i A(\tau)}{\sqrt{t-\tau}} d\tau$$

$$+ 2 \frac{kk_w}{\mu\sqrt{\pi\alpha}} \int_{\vartheta}^t \frac{p_*(\tau) - p_i A(\tau)}{\sqrt{t-\tau}} d\tau + 2 \frac{kk_w}{\mu\sqrt{\pi\alpha}} \int_{\vartheta}^t \frac{U(\tau)A(\tau)}{\sqrt{t-\tau}} d\tau. \quad (27)$$

In this setting, the control parameter is function  $U(t)$ . We have deliberately split the integral over  $[0, T]$  into two parts in order to single out the only term depending on the control parameter  $U(t)$ .

A perturbation  $\delta U(t)$  of the control parameter  $U(t)$  on interval  $[\vartheta, T]$  produces variation of functional (26) and constraint (27):

$$\delta J = \int_{\vartheta}^T w_q(t)V(t)\delta V(t)dt + \int_{\vartheta}^T w_p(t)U(t)\delta U(t)dt ; \dots(28)$$

$$\delta V(t) - 2 \frac{kk_w}{\mu\sqrt{\pi\alpha}} \int_{\vartheta}^t \frac{A(\tau)}{\sqrt{t-\tau}} \delta U(\tau)d\tau = 0 \dots\dots\dots(29)$$

The integral in Eq. (29) is taken only over  $[\vartheta, T]$  because the control variable  $U(t)$  is perturbed only on this interval and, by virtue of Eq. (27), this perturbation does not affect  $V(t)$  on  $[0, \vartheta]$ . Multiplying Eq. (29) by a Lagrange multiplier  $\psi(t)$ , integrating the result over  $[\vartheta, T]$  and adding to Eq. (28), one obtains:

$$\delta J = \int_{\vartheta}^T w_q(t)V(t) + \psi(t) \delta V(t)dt + \int_{\vartheta}^T w_p(t)U(t)\delta U(t)dt$$

$$- 2 \frac{kk_w}{\mu\sqrt{\pi\alpha}} \int_{\vartheta}^T \int_{\vartheta}^t \frac{A(\tau)}{\sqrt{t-\tau}} \delta U(\tau)d\tau dt. \quad (30)$$

After changing the order of iterated integration, one gets

$$\delta J = \int_{\vartheta}^T w_q(t)V(t) + \psi(t) \delta V(t)dt + \dots(31)$$

$$\int_{\vartheta}^T w_p(t)U(t) - 2 \frac{kk_w}{\mu\sqrt{\pi\alpha}} A(t) \int_{\vartheta}^t \frac{\psi(\tau)}{\sqrt{\tau-t}} d\tau \delta U(t)dt$$

The necessary and sufficient condition for a minimum in problem (26) - (27) is  $\delta J \geq 0$  for all arbitrarily small  $\delta U(t)$  and  $\delta V(t)$ . Hence, the minimum of functional (26) is characterized by the following system of equations:

$$\psi t = -w_q t V t ; \dots\dots\dots(32)$$

$$U t = 2 \frac{kk_w}{\mu\sqrt{\pi\alpha}w_p t} A t \int_{\vartheta}^t \frac{\psi \tau}{\sqrt{\tau-t}} d\tau \dots\dots(33)$$

By substituting  $\psi(t)$  from (32) into (33) and taking (27) into account, one finally obtains

$$V(t) = -Q_*(t) + wA(t) + 2 \frac{kk_w}{\mu\sqrt{\pi\alpha}} \int_{\vartheta}^t \frac{p_{inj}(\tau) - p_i A(\tau)}{\sqrt{t-\tau}} d\tau$$

$$+ 2 \frac{kk_w}{\mu\sqrt{\pi\alpha}} \int_{\vartheta}^t \frac{p_*(\tau) - p_i A(\tau)}{\sqrt{t-\tau}} d\tau + 2 \frac{kk_w}{\mu\sqrt{\pi\alpha}} \int_{\vartheta}^t \frac{U(\tau)A(\tau)}{\sqrt{t-\tau}} d\tau. \quad (27)$$

$$U(t) = -2 \frac{kk_w}{\mu\sqrt{\pi\alpha}w_p(t)} A(t) \int_{\vartheta}^t \frac{w_q(\tau)}{\sqrt{\tau-t}} V(\tau)d\tau, \quad \vartheta \leq t \leq T \dots(34)$$

If a pair of functions  $U_0(t), V_0(t)$  provides the solution to Eqs. (27) and (34), then in the original variables,  $p_{inj}(t) = p_*(t) + U_0(t)$  and  $Q(t) = Q_*(t) + V_0(t)$ , the optimal injection pressure and the cumulative injection policy are provided by

$$Q_0(t) = wA(t) + 2 \frac{kk_w}{\mu\sqrt{\pi\alpha}} \int_{\vartheta}^t \frac{p_{inj}(\tau) - p_i A(\tau)}{\sqrt{t-\tau}} d\tau ;$$

$$+ 2 \frac{kk_w}{\mu\sqrt{\pi\alpha}} \int_{\vartheta}^t \frac{p_0(\tau) - p_i A(\tau)}{\sqrt{t-\tau}} d\tau \dots\dots(35)$$

$$p_0 t = p_* t -$$

$$2 \frac{kk_w}{\mu\sqrt{\pi\alpha}w_p(t)} A(t) \int_0^t \frac{w_q(\tau)}{\sqrt{t-\tau}} Q_0(\tau) - Q_*(\tau) d\tau \dots\dots(36)$$

The importance of a nonzero weight function  $w_p(t)$  is now obvious. If this function vanishes, the injection pressure cannot be calculated from Eq. (36) and the controller output is not defined.

Equation (36), in particular, implies that the optimal injection pressure satisfies the condition  $p_0(T) = p_*(T)$ . The trivial function  $p_*(t) \equiv 0$  is not a good choice of the reference pressure in Eq. (25) because it enforces zero injection pressure by the end of the current subinterval. Another possibility  $p_*(t) \equiv p_i$  has the same drawback: it equalizes the injection pressure and the pressure outside the fracture by the end of the current interval. Apparently  $p_*(t)$  should exceed  $p_i$ . At the same time, too high a  $p_*(t)$  is not desirable because it may produce large overpressure and cause a catastrophic extension of the fracture. A rather simple and reasonable choice of  $p_*(t)$  is provided by  $p_*(t) \equiv P_*$ , where  $P_*$  is the optimal constant pressure on the interval  $[\vartheta, T]$ . The equation characterizing  $P_*$  will be obtained below. As soon as we have selected the reference function,  $p_*(t)$ , the optimal injection pressure is provided by solving Eqs. (35) - (36).

Note that the optimal cumulative injection,  $Q_0(t)$ , depends on the entire history of injection pressure up to time  $t$ . The optimal injection pressure depends on the current effective fracture area,  $A(t)$ , and on the deviation of the cumulative injection,  $Q_0(t)$ , from the reference injection,  $Q_*(t)$ . This feature of Eq. (36) causes some discomfort because the current optimal control depends on the data that will become available only in the future. There are several ways to circumvent this difficulty.

First, we can organize the process of control as a step-by-step procedure. We split the whole time interval into reasonably small parts, so that on each part one can make reasonable estimates of the required parameters. Then we compute the optimal injection pressure for this interval and apply it at the wellhead by adjusting the control valve. As soon as either the measured cumulative injection or the fracture area begins to deviate from the estimates used to determine the optimal injection pressure, the control interval  $[\vartheta, T]$  is refreshed. We must also revise our estimate of the fracture area,  $A(t)$ , for the refreshed interval and the expected optimal cumulative injection. In summary, the control is designed on a sliding time interval  $[\vartheta, T]$ . In order to circumvent the above-mentioned dependence on the future

data,  $p_{inj}(T) = p_*(T)$ , and the control interval is refreshed before the current interval ends even if the measured and computed parameters are in good agreement. Computer simulations show that even small overlap of control intervals considerably improves the controller performance.

Another possibility to resolve the difficulty in obtaining the optimal control from Eq. (36) is to change the model of fracture growth. So far, we have treated the fracture as a continuously growing object. On the other hand, it is clear that the rock surrounding the fracture is not a perfect elastic material and the area of the fracture grows in steps. This observation leads to the piecewise-constant fracture growth model. We may assume that the fracture area is constant on the current interval  $[\vartheta, T]$ . We have to be careful and if observation tells us that the fracture area has changed, the interval  $[\vartheta, T]$  must be adjusted, and control refreshed. Equations (35) and (36) are simpler for piecewise constant fracture area and this case is considered separately below.

Before discussing the model variations, let us make a remark concerning the solvability of the system of integral equations (35)-(36). For simplicity, let us assume that both weight functions  $w_p$  and  $w_q$  are constant. In this case, one may note that the integral operators on the right-hand sides of Eq. (35) and Eq. (36) are adjoint to each other. More precisely, if we define an integral operator

$$Df(\cdot)(t) = 2 \frac{kk_w}{\mu\sqrt{\pi\alpha}} \int_{\vartheta}^t \frac{f(\tau)A(\tau)}{\sqrt{t-\tau}} d\tau \dots\dots\dots(37)$$

then its adjoint operator is equal to

$$D^*g(\cdot)(t) = 2 \frac{kk_w}{\mu\sqrt{\pi\alpha}} A(t) \int_{\vartheta}^t \frac{g(\tau)}{\sqrt{t-\tau}} d\tau \dots\dots\dots(38)$$

The notation  $Df(\cdot)$  means that operator  $D$  transforms the whole function  $f(t)$ ,  $\vartheta \leq t \leq T$ , rather than its particular value, into another function defined on  $[\vartheta, T]$ , and  $Df(\cdot)(t)$  denotes the value of that other function at  $t$ . The notation  $Dg(\cdot)(t)$  is similar.

If both weight functions  $w_p$  and  $w_q$  are constant, then the system of equations (35), (36) can be expressed in the operator form as

$$\begin{cases} Q = DP + b_Q, \\ P = -\frac{w_q}{w_p} D^*Q + b_p, \end{cases} \dots\dots\dots(39)$$

where

$$b_Q(t) = wA(t) + 2 \frac{kk_w}{m\sqrt{\pi\alpha}} \int_0^t \frac{(p_{inj}(t) - p_i)A(t)}{\sqrt{t-\tau}} d\tau \dots\dots(40)$$

$$b_p(t) = p_s(t) + 2 \frac{w_q}{w_p} \frac{kk_w}{m\sqrt{pa}} A(t) \int_0^t \frac{1}{\sqrt{t-\tau}} Q_s(\tau) d\tau \dots(41)$$

and  $Q$  and  $P$  denote, respectively, the cumulative injection and injection pressure on the interval  $[\vartheta, T]$ . From Eq. (39) one deduces the following equation with one unknown function  $P$ :

$$D^* D + \frac{w_p}{w_q} Id \ P = -D^* b_Q + \frac{w_p}{w_q} b_p, \dots\dots\dots(42)$$

where  $Id$  is the identity operator. The operator inside the brackets on the left-hand side of Eq. (42) is self-adjoint and positive-definite. Therefore, the solution of Eq. (42) can be obtained with a conjugate gradient algorithm. Note that as the ratio  $\frac{w_p}{w_q}$  increases, the term  $\frac{w_p}{w_q} Id$  dominates Eq. (42), and

Eq. (42) becomes better posed. When  $w_p = 0$ , the second term in functional (26) must be dropped and in order to solve Eq. (42), one needs to invert a product of two Volterra integral operators. Although zero is not an eigenvalue of operator  $D$ , it is an element of its continuous spectrum<sup>19</sup> and, therefore, the problem of inversion of such an operator might be ill posed.

In the discretized form, operator  $D$  is a lower-triangular matrix; however, the product  $D^* D$  does not necessarily have a sparse structure. The above mentioned ill-posedness of the inversion of  $D$  manifests itself by the presence of a zero row in its discretization. Thus the rule: the larger is the ratio  $w_p/w_q$ , the better posed Eq. (42), holds true for the discretized form as well. However, if  $w_p/w_q$  is too large, then criterion (26) estimates the deviation of the injection pressure from  $p_s(t)$  on  $[\vartheta, T]$  rather than the ultimate objective of the controller. A reasonable choice in selecting the weights  $w_p$  and  $w_q$  should provide well-posedness of the system of integral equations (35)-(36) without substantial deviation from the control objectives.

**Control model for a layered reservoir**

Now let us consider a control problem in the situation described above, where there is water breakthrough in one or more layers of higher permeability. From Eq. (16) the total injection into the transient layers is given by

$$Q_T(t) = wA_T(t) + 2 \frac{K_T}{\mu\sqrt{\pi}} \int_0^t \frac{P_{inj}(\tau) - P_{init}}{\sqrt{t-\tau}} A(\tau) d\tau, \dots(43)$$

where

$$A_T(t) = \frac{1}{H} \sum_{i \in I} h_i A(t) \text{ and } K_T = \frac{1}{H} \sum_{i \in I} h_i \frac{k_i k_r}{\sqrt{\alpha_i}} \dots\dots\dots(44)$$

In order to estimate the largest possible injection on interval  $[\vartheta, T]$  under constraint (23), let us substitute Eq. (23) into Eq. (43):

$$Q_T^{\max}(t) = wA_T(t) + 2 \frac{K_T}{\mu\sqrt{\pi}} \int_0^\vartheta \frac{P_{inj}(\tau) - P_{init}}{\sqrt{t-\tau}} A(\tau) d\tau + \int_\vartheta^T \frac{P_{adm}(\tau) - P_{init}}{\sqrt{t-\tau}} A(\tau) d\tau \dots\dots\dots(45)$$

From Eq. (24), one obtains

$$Q_T^{\max}(t) = wA_T(t) + 2 \frac{K_T}{\mu\sqrt{\pi}} \int_0^\vartheta \frac{P_{inj}(\tau) - P_{init}}{\sqrt{t-\tau}} A(\tau) d\tau + \dots\dots\dots(46)$$

$$2 \frac{K_T}{\mu\sqrt{\pi}} \int_\vartheta^t \frac{(P_{pump}(\tau) - P_{init}) A(\tau)}{\sqrt{t-\tau}} d\tau + \frac{\sum_{i \in I} k_i k_r h_i}{\sum_{j \in J} k_j k_r h_j} q_{adm} L \sqrt{t-\vartheta} \cdot$$

Now let us analyze the right-hand side of Eq. (46). The first term expresses the fraction of the fracture volume that intersects the transient layers. Since the total volume of the fracture is small, this term is also small. The second term decays as  $\sqrt{\frac{\vartheta}{t}}$ , so if steady-state flow has been established by time  $\vartheta$ , the impact of this term is small as  $t \gg \vartheta$ . The main part of cumulative injection over a long time interval comes from the last two terms. Since production is possible only if

$$P_{pump} \ \tau < P_{init} \dots\dots\dots(47)$$

the third term is negative. Therefore, successful injection is possible without exceeding the admissible rate of injection into steady-state layers only if

$$\frac{\sum_{i \in I} k_i k_r h_i}{\sum_{j \in J} k_j k_r h_j} q_{adm} L \sqrt{t-\vartheta} > 2 \frac{k_r}{\mu\sqrt{\pi}} K_T \int_\vartheta^t \frac{P_{init} - P_{pump}(\tau)}{\sqrt{t-\tau}} A(\tau) d\tau \dots\dots(49)$$

After channeling has occurred, it is natural to assume that the fracture growth stops, since an increase of pressure will lead to circulating more water to the producers rather than to a fracture extension. In addition, we may assume that producers are pumped off at constant pressure, so that



$\Delta p_{pump} = p_{init} - p_{pump}(t)$  does not depend on  $t$ . Then condition (49) transforms into

$$q_{adm} HL > 2 \sum_{j \in J} \frac{k_j k_r h_j}{\mu} \Delta p_{pump} A_{\emptyset} \dots \dots \dots (50)$$

The latter inequality means that the area of the hydrofracture may not exceed the fatal threshold

$$A_{\emptyset} < \frac{q_{adm} HL}{2 \sum_{j \in J} \frac{k_j k_r h_j}{\mu} \Delta p_{pump}} \dots \dots \dots (51)$$

This conclusion can also be formulated in the following way. In a long run, the rate of injection into the steady-state layers,  $q_{chnt}$ , will be at least

$$q_{chnt} > \frac{2}{HL} \sum_{j \in J} \frac{k_j k_r h_j}{\mu} \Delta p_{pump} A_{\emptyset} \dots \dots \dots (52)$$

Therefore, smaller hydrofractures are better. In addition, a close injector-producer well spacing may increase the amount of channeled water. Indeed, in (51) the threshold of the fracture area is proportional to  $L$ , the distance to the neighboring producer.

## Nomenclature

- $A$  = effective fracture area,  $m^2$
- $F$  = fundamental solution, dimensionless
- $H$  = total thickness of injection interval,  $m$
- $h_i$  = thickness of layer  $i$ ,  $m$
- $k$  = absolute rock permeability,  $m^2$
- $k_r$  = relative permeability, dimensionless
- $K$  = average permeability,  $m^2$
- $L$  = distance between injector and producer,  $m$
- $l$  = fracture half length,  $m$
- $p_i$  = initial pressure in the formation outside the fracture,  $Pa$
- $p_{inj}$  = injection pressure,  $Pa$
- $q$  = injection rate,  $m^3/s$
- $Q$  = cumulative injection,  $m^3$
- $R$  = square root of time fracture growth rate,  $m/\sqrt{s}$
- $v$  = superficial leak-off velocity,  $m/s$
- $w$  = fracture width,  $m$
- $X$  = displacement distance,  $m$
- $\alpha$  = hydraulic diffusivity,  $m^2/s$
- $\phi$  = porosity, dimensionless
- $\mu$  = viscosity,  $Pa \cdot s$

## Conclusions

In this paper, we have implemented a model of water injection from an initially growing vertical hydrofracture into

layered rock. Initially, water injection is transient in each layer. The cumulative injection is then expressed by a sum of convolution integrals, which are proportional to the current and past area of the hydrofracture and the history of injection pressure. In transient flow, therefore, one might conclude that a bigger hydrofracture and higher injection pressure results in more injection and a faster waterflood. When injected water breaks through in one or more of the rock layers, the situation changes dramatically. Now a larger hydrofracture causes more water recirculation.

We have also proposed an optimal controller for transient and transient/steady-state water injection from a vertical hydrofracture into layered rock. We present three different modes of controller operation: the continuous mode, piecewise constant mode, and exactly optimal mode. The controller adjusts injection pressure to keep injection rate on target while the hydrofracture is growing. The controller can react to sudden hydrofracture extensions and prevent catastrophic ones. After water breakthrough occurs in some of the layers, we arrive at a condition for the maximum feasible hydrofracture area, beyond which waterflood may be uneconomic because of excessive recirculation of water.

In summary, we have coupled early transient behavior of water injectors with their later behavior after water breakthrough. We have shown that early water injection policy and the resulting hydrofracture growth may impact very unfavorably the later performance of the waterflood.

## Acknowledgements

This work was supported in part by two members of the U.C. Oil@ Consortium, Chevron Petroleum Technology Company, and Aera Energy, LLC. Partial support was also provided by the Assistant Secretary for Fossil Energy, Office of Gas and Petroleum Technology, under contract No. DE-AC03-76FS00098 to the Lawrence Berkeley National Laboratory of the University of California.

## References

1. Patzek, T.W., and Silin, D.B. *Water Injection into a Low-Permeability Rock - I. Hydrofracture Growth*, SPE 39698. in *11th Symposium on Improved Oil Recovery*. 1998. Tulsa, Oklahoma: Society of Petroleum Engineering.
2. De, A., and Patzek, T.W., "Waterflood Analyzer, MatLab Software Package," 1999, Lawrence Berkley National Lab: Berkeley, CA.
3. Holzhausen, G.R., and Gooch, R.P. *Impedance of Hydraulic Fractures: Its Measurement and Use for Estimating Fracture Closure Pressure and Dimensions*. in *SPE/DOE 1985 Conference on Low Permeability Gas Reservoirs*. 1985. Denver, CO: SPE.
4. Ashour, A.A.a.Y.C.H. *A study of the Fracture Impedance Method*. in *47th Annual CIM Petroleum Society Technical Meeting*. 1996. Calgary, Canada.
5. Patzek, T.W., and De, Asoke. *Lossy Transmission Line Model of Hydrofractured Well Dynamics*, in *1998 SPE Western Regional Meeting*. 1998. Bakersfield, CA: SPE.

6. Warpinski, N.R., "Hydraulic Fracture Diagnostics," *Journal of Petroleum Technology*, 1996(October).
7. Barenblatt, G.I., "On the Finiteness of Stresses at the Leading Edge of an Arbitrary Crack," *Journal of Applied Mathematics and Mechanics*, 1961. **25**(4): p. 1112-1115.
8. Murdoch, L.C., "Hydraulic Fracturing of Soil During Laboratory Experiments. Part 1 - Methods and observations," *Géotechnique*, 1992. **18**(2): p. 255-265.
9. Murdoch, L.C., "Hydraulic Fracturing of Soil during Laboratory Experiments. Part 3 - Theoretical Analysis," *Géotechnique*, 1992. **18**(2): p. 277-287.
10. Murdoch, L.C., "Hydraulic Fracturing of Soil during Laboratory Experiments. Part 2 - Propagation," *Géotechnique*, 1992. **18**(2): p. 267-276.
11. Barkman, J.H., and Davidson, D.H., "Measuring Water Quality and Predicting Well Impairment," *J. Pet. Tech.*, 1972(July): p. 865-873.
12. Patzek, T.W., and Silin, D.B., "Water Injection into a Low-Permeability Rock - 1. Hydrofracture Growth," *Transport in Porous Media*, 1999: p. Submitted.
13. Gordeyev, Y.N., Entov, V.M., "The Pressure Distribution around a Growing Crack," *J. Appl. Maths. Mechs.*, 1997. **51**(6): p. 1025-1029.
14. Settari, A., "Simulation of Hydraulic Fracturing Processes," *Society of Petroleum Engineers Journal*, 1980(December): p. 487-500.
15. Muskat, M., *The Flow of Homogeneous Fluids through Porous Media*. 1946, Ann Arbor, MI: J.W. Edwards, Inc.
16. Tikhonov, A.N., and Samarskii, A. A., *Equations of mathematical physics*. International series of monographs in pure and applied mathematics; v. 39. 1963, New York: Macmillan.
17. Tikhonov, A.N., and Arsenin, V. Y., *Solutions of ill-posed problems*. Scripta series in mathematics, ed. J. Fritz. 1977, New York: Halsted Press.
18. Vasil'ev, F.P., *Numerical Methods for Solving Extremal Problems (in Russian)*. 1982, Moscow: Nauka.
19. Kolmogorov, A.N., and Fomin, S. V., *Introductory Real Analysis*. 1975, New York: Dover Publications.

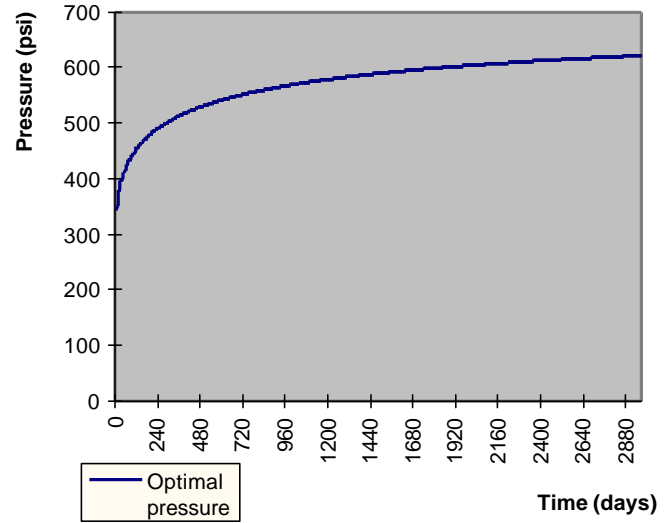


Fig. 2 - Optimal injection pressure when hydrofracture grows as the square root of time.

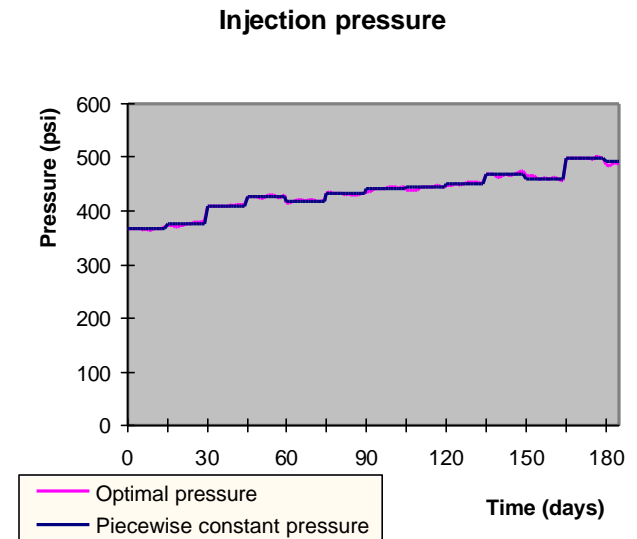


Fig. 3 - Optimal piecewise constant injection pressure if fracture area is estimated with random disturbances.

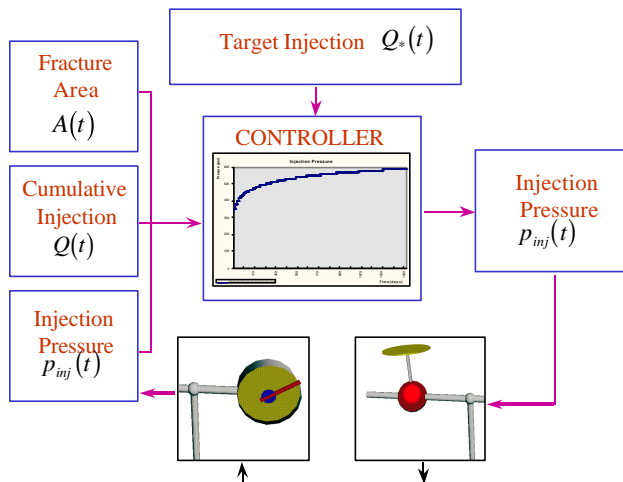


Fig. 1- The controller schematic.

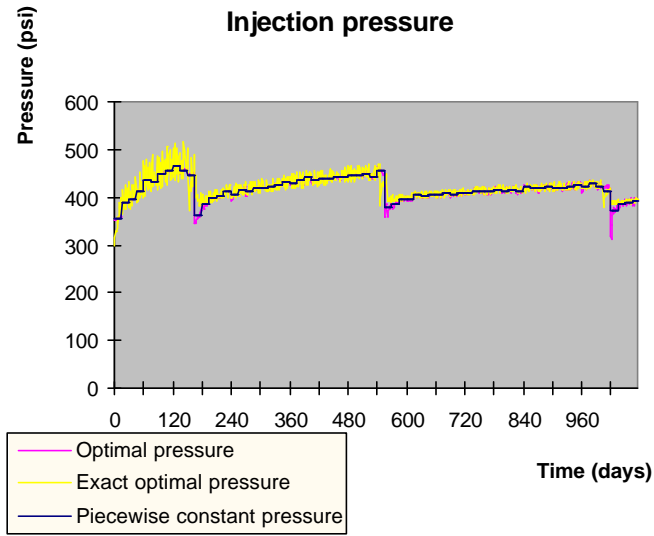


Fig. 4 - Three modes of optimal pressure when fracture area is measured with random disturbances and the fracture experiences extensions, also see Fig. 5.

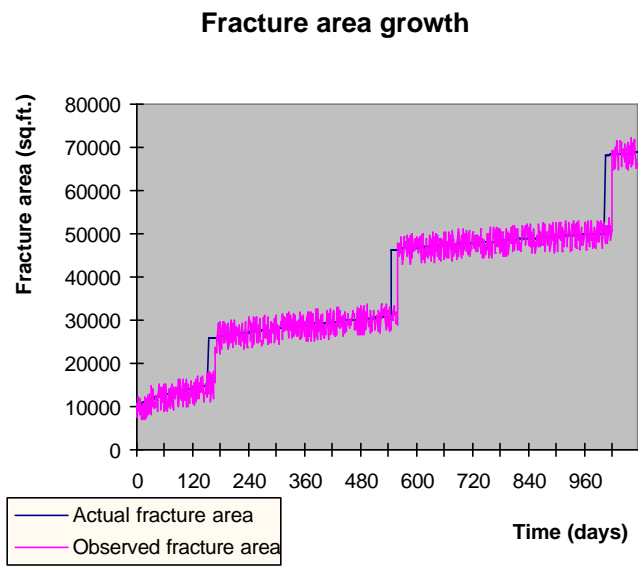


Fig. 5 - Fracture growth with several extensions. The hydrofracture area is measured with random noise.